

# CONSTANT FALSE ALARM RATE DETECTION IN SPHERICALLY INVARIANT RANDOM PROCESSES

F. Pascal<sup>1,2,3</sup>, J-P. Ovarlez<sup>1</sup>, P. Forster<sup>2</sup>, P. Larzabal<sup>3</sup>

<sup>1</sup> ONERA, Chemin de la Hunière, F-91761 Palaiseau Cedex, France

<sup>2</sup> GEA, 1 Chemin Desvallières, F-92410 Ville d'Avray, France

<sup>3</sup> ENS Cachan, 61 Avenue du Président Wilson, F-94235 Cachan Cedex, France

Email : pascal@onera.fr, ovarlez@onera.fr, philippe.forster@cva.u-paris10.fr, pascal.larzabal@satie.ens-cachan.fr

## ABSTRACT

In this paper, we use the theory of generalized likelihood ratio tests (GLRT) to study the adaptive version of the asymptotical Bayesian Optimum Radar Detector (BORD) built with a covariance matrix estimate. We investigate its properties, when the noise is modelled as a non-Gaussian complex process, such as Spherically Invariant Random Process (SIRP).

We derive, for appropriate covariance matrix estimates, the analytical expression of the relationship between the Probability of False Alarm (PFA) and the detection threshold. We show that this detector is SIRP-CFAR : the GLR distribution does not depend on the SIRP characteristics.

## 1. INTRODUCTION

Detection in non-Gaussian noise has gained many interests in the radar community. Indeed, since experimental clutter measurements made by organizations like MIT [1] showed that these data are correctly described by non-Gaussian statistical models. One of the most tractable and elegant non-Gaussian model comes from the so-called *Spherically Invariant Random Process* (SIRP) theory. A SIRP is the product of a Gaussian random process - called *speckle* - with a non-negative random variable - called *texture*. This model leads to many results [2, 3, 4, 5, 6, 7]. For example, Gini et al.'s have derived in [7], the optimum detector in the presence of a SIRP noise with known statistics.

In previous works [8, 9], a bayesian approach was proposed to determine the PDF of the *texture* (the SIRP characteristic PDF) from  $N$  reference clutter cells. It allowed to derive the expression of the optimum detector called Bayesian Optimum Radar Detector (BORD). For all the SIRPs, the BORD does not require the knowledge of the PDF texture and nevertheless reaches the performances of the Neyman-Pearson detector with known noise statistic. Moreover BORD was shown to be an adaptive detector : it is so no more necessary to have any knowledge about the clutter statistics but BORD deals directly with the received data.

## 2. PROBLEM STATEMENT AND BACKGROUND

We consider here the basic problem of detecting a complex signal  $\mathbf{s}$  corrupted by an additive SIRP noise  $\mathbf{c}$  (clutter) in a  $m$ -dimensional complex vector  $\mathbf{y}$ . This can be stated as the following binary hypothesis test :

$$\begin{cases} H_0 : \mathbf{y} = \mathbf{c} & \mathbf{y}_i = \mathbf{c}_i \quad i = 1, \dots, N \\ H_1 : \mathbf{y} = \mathbf{s} + \mathbf{c} & \mathbf{y}_i = \mathbf{c}_i \quad i = 1, \dots, N \end{cases} \quad (1)$$

where  $\mathbf{y}_i$  are  $N$  signal-free independent measurements which will be used to estimate clutter covariance matrix.

Under the hypothesis  $H_1$ , it is instead assumed that the observed data consist in the sum of a signal  $\mathbf{s} = \alpha \mathbf{p}$  and clutter  $\mathbf{c}$ , where  $\mathbf{p}$  is a perfectly known complex steering vector and  $\alpha$  is the signal complex amplitude.

The clutter is modelled as a SIRP, a non-homogeneous Gaussian process with random power : its randomness is induced by spatial variation in the radar backscattering. A SIRP [10] is the product of a positive random variable  $\tau$  (*texture*), and a  $m$ -dimensional independent complex Gaussian vector  $\mathbf{x}$  (*speckle*), with zero mean and normalized covariance matrix  $\mathbf{M} = \mathbb{E}(\mathbf{x}\mathbf{x}^\dagger)$  with  $\mathbf{M}_{ii} = 1$ , where  $\dagger$  denotes the conjugate transpose operator :

$$\mathbf{c} = \sqrt{\tau} \mathbf{x} .$$

The SIRP PDF expression is recalled :

$$p_m(\mathbf{c}) = \int_0^{+\infty} g_m(\mathbf{c}, \tau) p(\tau) d\tau , \quad (2)$$

where

$$g_m(\mathbf{c}, \tau) = \frac{1}{(2\pi\tau)^{m/2} \sqrt{|\mathbf{M}|}} \exp\left(-\frac{\mathbf{c}^\dagger \mathbf{M}^{-1} \mathbf{c}}{2\tau}\right) . \quad (3)$$

Let us consider the classical likelihood ratio for the detection problem (1) :

$$\Lambda(\mathbf{y}) = \frac{p(\mathbf{y}/H_1)}{p(\mathbf{y}/H_0)} \underset{H_0}{\overset{H_1}{\gtrless}} \eta , \quad (4)$$

For given range cell and steering vector  $\mathbf{p}$ , this detection test involves the following unknown quantities : the amplitude  $\alpha$ , the texture PDF  $p(\tau)$  and the covariance matrix  $\mathbf{M}$ . Therefore, a Generalized Likelihood Ratio Test (GLRT) is usually developed. The major difficulty comes from the estimation of the texture PDF. When  $\mathbf{M}$  is known, this problem was solved in a different way in [8, 9] (BORD) and [3, 4] (GLRT - Linear Quadratic (GLRT-LQ)).

For the BORD,  $p(\mathbf{y}/H_1)$  and  $p(\mathbf{y}/H_0)$  were replaced by their Bayesian estimates. Asymptotically, BORD tends to asymptotical BORD (aBORD) leading to the test :

$$\Lambda = \frac{|\mathbf{p}^\dagger \mathbf{M}^{-1} \mathbf{y}|^2}{(\mathbf{p}^\dagger \mathbf{M}^{-1} \mathbf{p})(\mathbf{y}^\dagger \mathbf{M}^{-1} \mathbf{y})} \underset{H_0}{\overset{H_1}{\gtrless}} \lambda , \quad (5)$$

with  $\lambda = 1 - \eta^{-\frac{1}{m}}$ .

The aBORD properties were studied in [9]. In particular, it has the CFAR property with regard to the *texture* distribution (i.e. it remains independent whatever the texture distribution).

This is illustrated on the following figure which represents the relation between the detection threshold  $\eta$  and the Probability of False Alarm  $P_{fa}$  for different SIRP distribution : Gaussian, K-distribution, Student-t and SIRP with a Weibull *texture*.

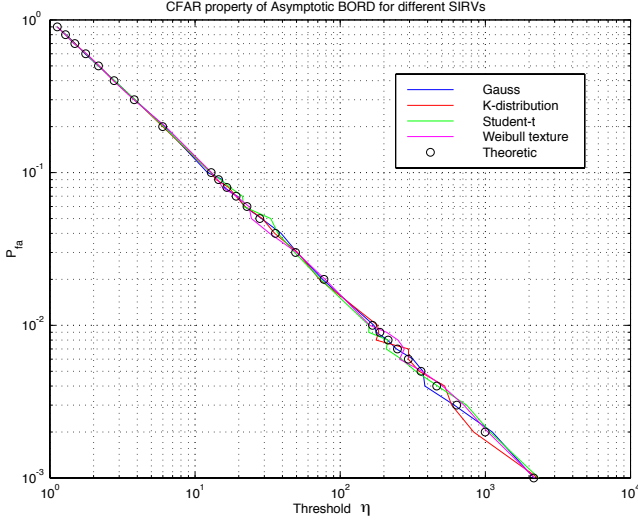


Figure 1: CFAR property for the aBORD when the covariance matrix is perfectly known

The relationship between the Probability of False Alarm  $P_{fa}$  defined by :

$$P_{fa} = \mathbb{P}(\Lambda > \lambda / H_0),$$

and the detection threshold  $\eta$  (or  $\lambda$ ) leads to :

$$\eta = P_{fa}^{\frac{m}{1-m}}, \quad \lambda = 1 - P_{fa}^{-\frac{1}{1-m}}. \quad (6)$$

In practice,  $\mathbf{M}$  is generally unknown and quite difficult to obtain. Hence it has to be estimated from  $\mathbf{y}_i$  data.

Test (5), rewritten in terms of estimated covariance matrix  $\hat{\mathbf{M}}$ , provides the so-called adaptive version of the aBORD :

$$\hat{\Lambda}(\hat{\mathbf{M}}) = \frac{|\mathbf{p}^\dagger \hat{\mathbf{M}}^{-1} \mathbf{y}|^2}{(\mathbf{p}^\dagger \hat{\mathbf{M}}^{-1} \mathbf{p})(\mathbf{y}^\dagger \hat{\mathbf{M}}^{-1} \mathbf{y})} \underset{H_0}{\overset{H_1}{\geq}} \lambda, \quad (7)$$

where we have emphasized the functional dependence of  $\hat{\Lambda}$  on the covariance estimator  $\hat{\mathbf{M}}$ .

The major contribution of this paper is to establish the distribution of  $\hat{\Lambda}(\hat{\mathbf{M}})$  for several estimators  $\hat{\mathbf{M}}$ .

### 3. ADAPTIVE DETECTION PERFORMANCES

We will start with the normalized sample covariance matrix estimate (NSCME) first proposed in [11] and defined as follows :

$$\hat{\mathbf{M}}_{NSCME} = \frac{m}{N} \sum_{i=1}^N \left( \frac{\mathbf{c}_i \mathbf{c}_i^\dagger}{\mathbf{c}_i^\dagger \mathbf{c}_i} \right). \quad (8)$$

Denominator is used to normalize each term of the sample covariance matrix estimate by the SIRP power.

$\hat{\mathbf{M}}_{NSCME}$  defined by (8) is statistically independent of the *texture* distribution :

$$\hat{\mathbf{M}}_{NSCME} = \frac{m}{N} \sum_{i=1}^N \left( \frac{\mathbf{c}_i \mathbf{c}_i^\dagger}{\mathbf{c}_i^\dagger \mathbf{c}_i} \right) = \frac{m}{N} \sum_{i=1}^N \left( \frac{\mathbf{x}_i \mathbf{x}_i^\dagger}{\mathbf{x}_i^\dagger \mathbf{x}_i} \right). \quad (9)$$

This feature is significant and is referred to as the texture-CFAR property. However, it can be shown that the test distribution depends on the covariance matrix  $\mathbf{M}$  : the resulting test is not  $\mathbf{M}$ -CFAR. Nevertheless, when  $m$  tends to infinity,  $\mathbf{x}_i^\dagger \mathbf{x}_i / m$  tends to one. Therefore, it is interesting to study  $\hat{\Lambda}(\hat{\mathbf{M}}_w)$  when  $\hat{\mathbf{M}}_w$  is the sample Gaussian covariance matrix :

$$\hat{\mathbf{M}}_w = \frac{1}{N} \sum_{i=1}^N \mathbf{x}_i \mathbf{x}_i^\dagger, \quad (10)$$

which is complex Wishart-distributed.

#### 3.1 $\hat{\Lambda}(\hat{\mathbf{M}}_w)$ distribution

The starting point [12] for the derivation of  $\hat{\Lambda}(\hat{\mathbf{M}}_w)$  PDF is based on Wishart's theory. Kraut, in [12] rewrites  $\hat{\Lambda}(\hat{\mathbf{M}}_w)$  defined by (7) in terms of random variable  $\hat{F}$  :

$$\hat{\Lambda}(\hat{\mathbf{M}}_w) = \frac{\hat{F}}{\hat{F} + 1},$$

where  $\hat{F}$  depends on another random variable  $B$ . Conditionally to  $B$ ,  $\hat{F}$  is  $\beta_{1, N_r, -m+1}^2$ -distributed and  $B$  is  $\beta_{N_r - m + 2, m-1}^1$ -distributed, with  $\beta_{a,b}^1$  and  $\beta_{a,b}^2$  PDF defined by [13] :

$$\beta_{a,b}^1(x) = \frac{\Gamma(a+b)}{\Gamma(a)\Gamma(b)} x^{a-1} (1-x)^{b-1} \Pi_{[0,1]}(x),$$

and

$$\beta_{a,b}^2(x) = \frac{\Gamma(a+b)}{\Gamma(a)\Gamma(b)} \frac{x^{a-1}}{(1+x)^{a+b}}, \quad x > 0$$

where  $\Pi_{[0,1]}(x)$  is the window function on the interval  $[0, 1]$ . After several basic probabilistic considerations, we obtain the following original results :

- the adaptive GLR  $\hat{\Lambda}(\hat{\mathbf{M}}_w)$  is distributed according to :

$$g_{N,m}(x) = \frac{(N-m+1)(m-1)}{(N-1)} \frac{{}_2F_1(a, a; b; x)}{(1-x)^{N-m}} \Pi_{[0,1]}(x)$$

where  $a = N - m + 2$ ,  $b = N + 2$  and  ${}_2F_1$  is the hypergeometric function [13] defined as :

$${}_2F_1(a, b; c; x) = \frac{\Gamma(c)}{\Gamma(a)\Gamma(b)} \sum_{k=0}^{\infty} \frac{\Gamma(a+k)\Gamma(b+k)}{\Gamma(c+k)} \frac{x^k}{k!}.$$

- the relationship between the threshold  $\eta$  (or  $\lambda$ ) and  $P_{fa}$  is given by :

$$\begin{aligned} P_{fa} &= \eta^{-\frac{a-1}{m}} {}_2F_1\left(a, a-1; b-1; 1-\eta^{-\frac{1}{m}}\right) \quad (11) \\ &= (1-\lambda)^{a-1} {}_2F_1(a, a-1; b-1; \lambda) \end{aligned}$$

Figure 2 validates the theoretical relationship (11) by the Monte-Carlo method for  $m = 10$  and various values of  $N$ . The dashed line is obtained from the relationship (6) where the covariance matrix  $\mathbf{M}$  is perfectly known.

As expected, the Monte-Carlo simulations confirm the theoretical result given by (11). Moreover, since the covariance matrix estimate (10) tends to the true covariance matrix  $\mathbf{M}$  when  $N$  tends to infinity, we also have the convergence in probability of  $\hat{\Lambda}(\hat{\mathbf{M}}_w)$  to the aBORD (5) :

$$\mathbb{P}(\hat{\Lambda}(\hat{\mathbf{M}}_w) > \lambda) \xrightarrow[N \rightarrow \infty]{} \mathbb{P}(\Lambda > \lambda).$$

As a consequence, when  $N$  tends to infinity, there is a convergence of (11) to (6), as shown on figure 2.

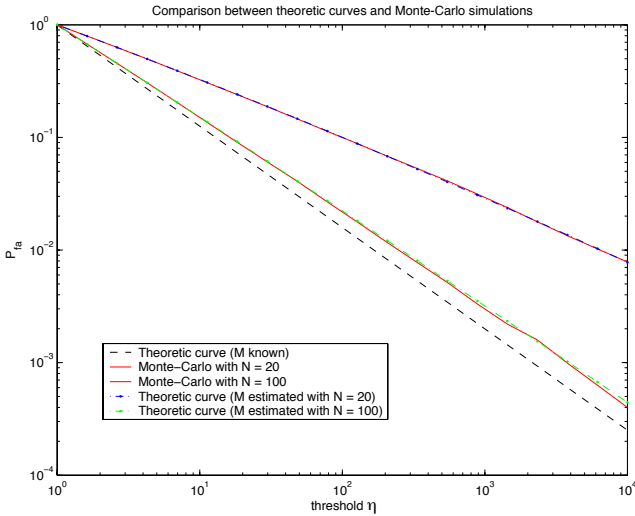


Figure 2: Validation of the relation (11) for different values of  $N$

### 3.2 An improved estimator $\hat{\mathbf{M}}_{fp}$

Despite of its interesting properties, the NSCME (8) suffers the following drawbacks :

- it is a biased estimate;
- the resulting adaptive GLR  $\hat{\Lambda}(\hat{\mathbf{M}}_{NSCME})$  is not  $\mathbf{M}$ -CFAR.

Recently, a recursive estimation of the covariance matrix has been introduced in [14] as a numerical procedure for computing the Maximum Likelihood of  $\mathbf{M}$  :

$$\hat{\mathbf{M}}_{t+1} = \frac{m}{N} \sum_{i=1}^N \left( \frac{\mathbf{c}_i \mathbf{c}_i^\dagger}{\mathbf{c}_i^\dagger \hat{\mathbf{M}}_t^{-1} \mathbf{c}_i} \right). \quad (12)$$

In this section, we derive new properties of this estimator. These properties are of a great interest for our detection problem. Let the function  $f$  be defined from the recursive relation (12) :

$$f(\hat{\mathbf{M}}) = \frac{m}{N} \sum_{i=1}^N \left( \frac{\mathbf{c}_i \mathbf{c}_i^\dagger}{\mathbf{c}_i^\dagger \hat{\mathbf{M}}^{-1} \mathbf{c}_i} \right). \quad (13)$$

**Theorem 1** We have the following results

1. the function  $f$  admits a single fixed point, called  $\hat{\mathbf{M}}_{fp}$ ;
2.  $\hat{\mathbf{M}}_t \rightarrow \hat{\mathbf{M}}_{fp}$ ;
3. the estimate  $\hat{\mathbf{M}}_{fp}$  is not biased;
4. the GLR  $\hat{\Lambda}(\hat{\mathbf{M}}_{fp})$  is texture-CFAR for all SIRPs;
5. the GLR  $\hat{\Lambda}(\hat{\mathbf{M}}_{fp})$  is  $\mathbf{M}$ -CFAR for all SIRPs.

**Proof 1** Proofs are too long to fit in this paper and will be developed in a forthcoming paper.

We will call SIRP-CFAR detector, a detector which verifies the two points 4 and 5 of the above theorem.

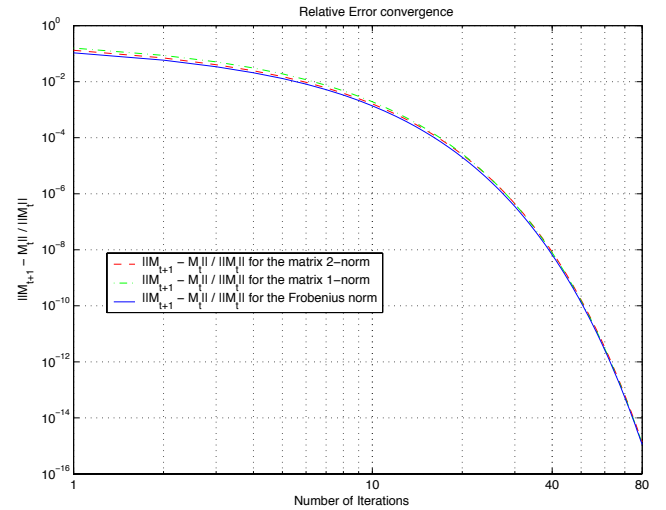


Figure 3: Illustration of the convergence to the fixed point.

Figure 3 illustrates the second point of the above theorem. On this figure, the relative error  $\|f(\hat{\mathbf{M}}_t) - \hat{\mathbf{M}}_t\| / \|\hat{\mathbf{M}}_t\|$  has been plotted versus  $t$  with initial value  $\hat{\mathbf{M}}_0 = \hat{\mathbf{M}}_{NSCME}$  (8).

Other simulations have been performed with different initial values  $\hat{\mathbf{M}}_0$  (ex : sample Gaussian covariance estimate, matrix with uniform PDF, deterministic Toeplitz ma-

trix), each of them conducting to the same value with an extremely fast convergence :

$$\|\mathbf{f}(\widehat{\mathbf{M}}_t) - \widehat{\mathbf{M}}_t\| \xrightarrow[t \rightarrow \infty]{} 0$$

### 3.3 Study of $\hat{\Lambda}(\widehat{\mathbf{M}}_{fp})$ behavior

In this section, we analyze by Monte-Carlo simulations the relationship between the Probability of False Alarm and the threshold for the GLR  $\hat{\Lambda}(\widehat{\mathbf{M}}_{fp})$ .

Figure 4 presents Monte-Carlo simulations. On this figure, the dependance between the threshold and the PFA has been displayed for different SIRP distribution : Gaussian, K-distribution, Student-t, Cauchy, Laplace.

One can observe that the relationship (11) between the threshold and the PFA, found in the special case where the covariance matrix estimate is Wishart-distributed, seems to be valid even if the SIRP is not Gaussian when taking for  $\widehat{\mathbf{M}}$  the fixed point of  $f$ .

Therefore, remarkably, the Monte-Carlo simulations show that all the GLR  $\hat{\Lambda}(\widehat{\mathbf{M}}_{fp})$  follow the same distribution than the  $\hat{\Lambda}(\widehat{\mathbf{M}}_w)$ 's one. Hence, we infer that the relationship (11) remains valid for  $\hat{\Lambda}(\widehat{\mathbf{M}}_{fp})$  although we have not yet proved this assertion.

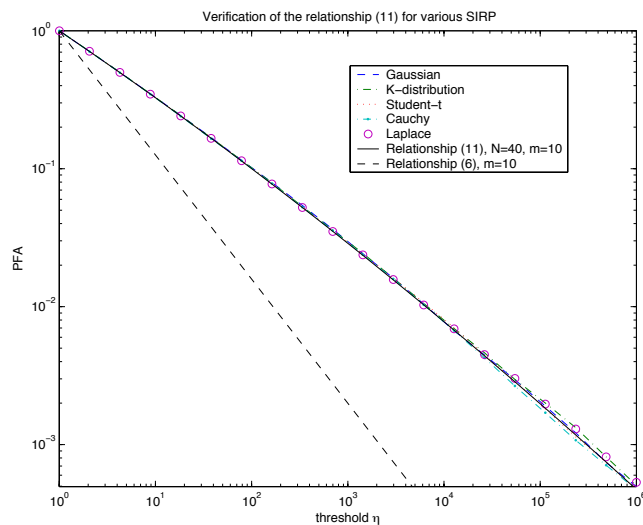


Figure 4:  $\hat{\Lambda}(\widehat{\mathbf{M}}_{fp})$  CFAR property for different SIRPs

## 4. CONCLUSION

In this paper, we have studied the adaptive GLRT (BORD) when the SIRP covariance matrix is estimated. We have first derived the distribution of the adaptive BORD in the Gaussian case using the sample covariance matrix. Although this case is restrictive in our non-Gaussian context, we have shown through extensive simulations that this distribution seems to be valid in a non-Gaussian noise (SIRP) when using an appropriate covariance matrix estimate.

The resulting detector has the following important property : it is SIRP-CFAR (invariance of its distribution with respect to the texture and to the speckle covariance matrix).

Moreover, this estimate was shown to be unbiased, to be the fixed point of a suitable function and to be the limit of a recurrence relation.

## REFERENCES

- [1] J.B. Billingsley, Ground Clutter Measurements for Surface-Sited Radar, *Technical Report 780, MIT*, February 1993.
- [2] T.J. Barnard and D.D. Weiner, Non-Gaussian Clutter Modeling with Generalized Spherically Invariant Random Vectors, *IEEE Trans.-SP*, **44**(10) (October 1996), 2384-2390.
- [3] E. Conte, M. Lops and G. Ricci, Asymptotically Optimum Radar Detection in Compound-Gaussian Clutter, *IEEE Trans.-AES*, **31**(2) (April 1995), 617-625.
- [4] F. Gini, Sub-Optimum Coherent Radar Detection in a Mixture of K-Distributed and Gaussian Clutter, *IEE Proc.Radar, Sonar Navig*, **144**(1) (February 1997), 39-48.
- [5] F. Gini and M.V. Greco, Sub-Optimum Approach to Adaptive Coherent Radar Detection in Compound-Gaussian Clutter, *IEEE Trans.-AES*, **35**-3 (July 1999), 1095-1103.
- [6] K.J. Sangston, F. Gini, M.V. Greco and A. Farina, Structures for Radar Detection in Compound Gaussian Clutter, *IEEE Trans.-AES* **35**(2) (April 1999), 445-458
- [7] F. Gini, M.V. Greco, A. Farina and P. Lombardo, Optimum and Mismatched Detection Against K-distributed Clutter Plus Gaussian Clutter, *IEEE Trans.-AES*, **34**(3) (July 1998), 860-876.
- [8] E. Jay, J.P. Ovarlez, D. Declercq and P. Duvaut, BORD : Bayesian Optimum Radar Detector, *Signal Processing*, **83**(6) (June 2003), 1151-1162
- [9] E. Jay, Détection en Environnement non-Gaussien, *Ph.D. Thesis*, University of Cergy-Pontoise / ONERA, France, June 2002.
- [10] K. YAO "A Representation Theorem and its Applications to Spherically Invariant Random Processes", *IEEE Trans.-IT*, Vol.19, No.5, pp.600-608 Sept. 1973
- [11] E. CONTE AND G. RICCI, "Performance Prediction in Compound-Gaussian Clutter", *IEEE Trans.-AES*, Vol.30, No.2, pp.611-616, April 1994
- [12] S. KRAUT , L.L. SCHARF AND L.T. MC WHORTER, "Adaptive Subspace Detectors", *IEEE*, January 2001
- [13] M. ABRAMOWITZ AND I.A. STEGUN, "Handbook of Mathematical Functions", National Bureau of Standard, AMS 55, June 1964
- [14] E. CONTE, A. DE MAIO AND G. RICCI, "Recursive Estimation of the Covariance Matrix of a Compound-Gaussian Process and Its Application to Adaptive CFAR Detection", *IEEE Trans.-SP*, Vol.50, No.8, pp.1908-1915, August 2002